Pathways for hydrogen desorption from $Si_{1-x}Ge_x(001)$ during gas-source molecular-beam epitaxy and ultrahigh-vacuum chemical vapor deposition

H. Kim, P. Desjardins, J. R. Abelson, and J. E. Greene
Materials Science Department, the Coordinated Science Laboratory, and the Materials Research Laboratory, University of Illinois, 1101 West Springfield Avenue, Urbana, Illinois 61801

(Received 29 December 1997)

D_2 temperature-programmed desorption (TPD) has been used to probe pathways for hydrogen desorption from $Si_{1-x}Ge_x(001)$ surfaces. The experiments were performed on Ge-adsorbed Si(001), Si-adsorbed Ge(001), and $Si_{1-x}Ge_x(001)$ alloy layers grown on Si(001). The depositions were done in ultrahigh vacuum using Si_2H_6 and Ge_2H_6 gaseous precursors. Immediately following partial monolayer or alloy film growth (and, in some cases, postdeposition annealing), the samples were quenched to <200 °C, H exchanged for D, and D_2 TPD carried out *in situ*. All TPD peaks were fit using standard Polanyi-Wigner desorption models. Both the Si and the Ge monodeuteride desorption energies were found to decrease linearly with increasing Ge coverage. In addition, a comparison of adsorbed-layer and alloy film results shows that deuterium desorption energies depend not just upon the surface-layer Ge coverage, but on second-layer Ge concentration as well. Finally, we show that, in contrast to some previous models, hydrogen desorption from Si sites occurs directly, rather than via diffusion to and subsequent desorption from lower-binding energy Ge sites. We briefly discuss the consequences of these results for modeling gas-source $Si_{1-x}Ge_x$ growth kinetics. [S0163-1829(98)07632-2]

I. INTRODUCTION

$Si_{1-x}Ge_x/Si$ heterostructures are of interest for device applications incorporating both band-gap engineering and the lower hole[1] (electron[2]) effective masses, and hence higher hole (electron) mobilities, associated with $Si_{1-x}Ge_x$ layers strained in compression (tension). Heterojunction bipolar transistors utilizing *p*-type $Si_{1-x}Ge_x$ base layers have been shown to have higher current gains and faster switching speeds, up to 100 GHz,[3] than obtained with Si homojunction devices. Other applications include modulation-doped field-effect transistors[4,5] and infrared detection devices.[6]

Gas-source molecular-beam epitaxy (GS-MBE) and ultrahigh-vacuum chemical vapor deposition (UHV-CVD) offer advantages over solid-source MBE for the growth of Si and $Si_{1-x}Ge_x$. These include the elimination of high-temperature evaporation sources, higher sample throughput, and better conformal coverage.[7] One potential disadvantage is that the kinetics of gas-source $Si_{1-x}Ge_x$ growth are complex and directly dependent upon both hydrogen desorption and Ge surface segregation rates, which are themselves interlinked.[8] Previous temperature-programmed desorption[9] (TPD) and IR spectroscopy[10] studies carried out on Ge-adsorbed Si(001) have shown qualitatively that the activation energy for hydrogen desorption decreases with increasing Ge coverage θ_{Ge}. However, no quantitative data are available. Unanswered questions include the primary hydrogen desorption site serving as the rate-limiting step during low-temperature gas-source $Si_{1-x}Ge_x$ growth and the role of Ge surface segregation.

We have recently used D_2 TPD to determine Ge segregation rates, and enthalpies, as a function of bulk film composition, steady-state hydrogen surface coverage θ_H, and deposition temperature T_s during GS-MBE growth of $Si_{1-x}Ge_x(001)$ from Si_2H_6/Ge_2H_6 mixtures.[8] In this article, we report results from experiments designed to probe the pathway for hydrogen desorption from $Si_{1-x}Ge_x(001)$ surfaces. For these studies, Ge-adsorbed Si(001), Si-adsorbed Ge(001), and $Si_{1-x}Ge_x(001)$ alloy surfaces were prepared by GS-MBE from Si_2H_6 and/or Ge_2H_6 exposures as a function of temperature. TPD was then used to quantitatively determine hydrogen desorption energies as a function of Ge coverage θ_{Ge}. The results show that both the Si and the Ge monohydride desorption energies decrease linearly with increasing θ_{Ge} and establish that the desorption energies also depend sensitively upon second-layer composition. Finally, we demonstrate that the rate-limiting step for gas-source $Si_{1-x}Ge_x$ film growth from hydride precursors is H desorption directly from Si sites rather than diffusion to lower-binding-energy Ge sites and desorption from there as initially proposed.[10,11]

II. EXPERIMENTAL PROCEDURE

The experiments were carried out in a four-chamber ultrahigh-vacuum system, described in Ref. 12, with a base pressure of 5×10^{-11} Torr. The film growth chamber, which is equipped with reflection high-energy electron diffraction (RHEED) and a quadrupole mass spectrometer (QMS), is connected through a transfer chamber to an analytical station containing provisions for Auger electron spectroscopy (AES), electron-energy-loss spectroscopy, and low-energy electron diffraction. TPD measurements were performed in a separate chamber attached to the analytical station and containing a heavily differentially pumped Extrel QMS. The final chamber contains a scanning tunneling microscope.

Three different types of samples were analyzed in these experiments. The first two consisted of partial monolayers of Ge on Si(001) and Si on Ge(001) obtained by exposing clean substrates to controlled doses of Ge_2H_6 or Si_2H_6 at temperatures ranging from 200 to 300 °C to provide coverages be-

0163-1829/98/58(8)/4803(6)/$15.00 PRB 58 © 1998 The American Physical Society

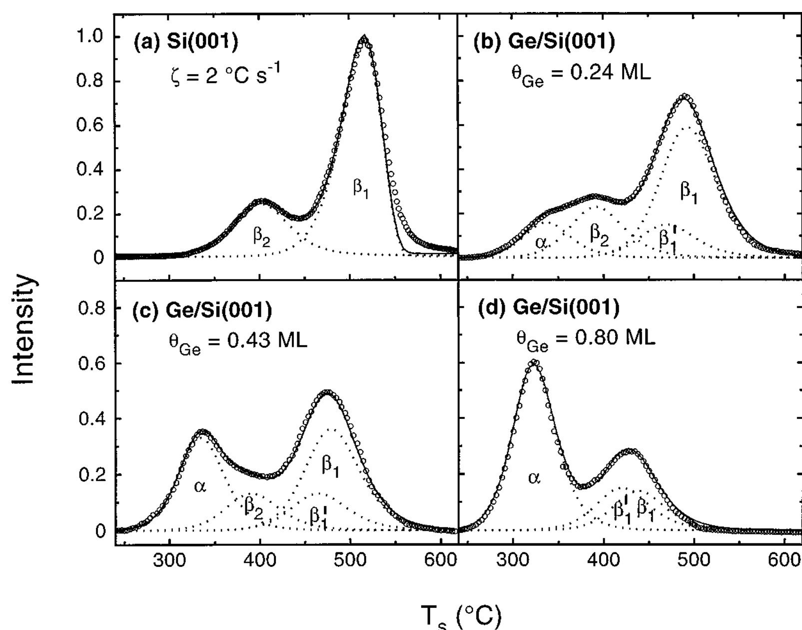

FIG. 1. D_2 TPD spectra from (a) Si(001) and (b)–(d) Ge-adsorbed Si(001) surfaces with Ge coverages θ_{Ge} of (b) 0.24, (c) 0.43, and (d) 0.80 ML. The adsorbed-layer samples were prepared by Ge_2H_6 dosing with a flux $J_{Ge_2H_6}=5\times10^{14}$ cm^{-2} s^{-1} for 5 min at (b) 200 °C, (c) 300 °C, and (d) 400 °C.

tween 0.2 and 1 ML. The third set of samples were $Si_{1-x}Ge_x(001)$ alloys, with x up to 0.18, grown on Si(001) by GS-MBE at $T_s=400$–500 °C. In all cases, the Si_2H_6 and Ge_2H_6 fluxes were delivered through tubular dosers located 3 cm from the substrate at an angle of 45°. The dosers are coupled to feedback-controlled constant-pressure reservoirs in which pressures are separately monitored by capacitance manometers whose signals are used to control variable leak valves. Following adlayer or alloy deposition (and, in some cases, postdeposition annealing), the samples were quenched to <200 °C and exposed to atomic deuterium. For this purpose, D_2 was delivered through a doser identical to those described above, but with a hot W filament near the outlet to crack the gas. All hydrogen was exchanged for D as demonstrated by TPD.

For the TPD experiments, the as-deposited sample was placed 2 mm from the 5-mm-diameter hole in the skimmer cone between the mass spectrometer and analytical chambers. Samples were heated at a linear rate ζ, typically $\zeta=2$ °C s^{-1}, by direct current while the temperature was measured using a thermocouple calibrated with an optical pyrometer.

The Si(001) substrates were 1×3 cm^2 plates cleaved from 0.5-mm-thick n-type $[n=(1-2)\times10^{14}$ cm$^{-3}]$ wafers. Initial cleaning consisted of solvent degreasing, multiple wet-chemical oxidation/etch cycles, and a 20-s etch in dilute (10%) HF.[12] The substrates were then exposed to a UV/ozone treatment to remove C-containing species[13] and introduced through the sample-exchange chamber, into the deposition system where they were degassed at 600 °C for 4 h and then rapidly heated at 100 °C s^{-1} to 1100 °C for 1 min to desorb the oxide layer. The 1×3-cm^2 n-type $[n=(1-5)\times10^{14}$ cm$^{-3}]$ Ge(001) substrates were cleaned following a similar procedure except that the etch was carried out in deionized water while UHV degassing and final oxide desorption were done at 300 °C for 8 h and 500 °C for 1 min, respectively. RHEED patterns from Si and Ge substrates subjected to these procedures were 2×1 with sharp Kikuchi lines. No residual C or O was detected by AES.

Prior to adlayer or alloy film growth, ≃400-nm-thick Si (Ge) buffer layers were grown on the clean Si(001) [Ge(001)] substrates at 800 °C (325 °C). RHEED patterns remained 2×1, but now consisted of well-defined diffraction spots, rather than streaks, indicating atomically smooth surfaces with relatively large terraces. RHEED patterns from $Si_{1-x}Ge_x$ overlayers with $x\leqslant0.08$ remained 2×1 while patterns obtained from layers with higher Ge concentrations corresponded to ordered $2\times n$ surface superstructures due to dimer vacancy reconstructions.[8] In both cases, the patterns exhibited well-defined diffraction spots characteristic of smooth surfaces.

III. EXPERIMENTAL RESULTS

Figure 1 shows typical D_2 TPD spectra from Ge-adsorbed Si(001) surfaces with coverages θ_{Ge} (determined as discussed below) of (a) 0, (b) 0.24, (c) 0.43, and (d) 0.80 ML. D_2 TPD spectra from clean Si(001) consist of peaks, labeled β_2 and β_1, centered at 405 and 515 °C due to desorption from the 1×1 dideuteride phase and the 2×1 monodeuteride phase, respectively.[14] While β_2 desorption is second order, β_1 follows first-order kinetics, except at very low deuterium coverages $\theta_D<0.1$ ML,[15] due to π-bonding-induced pairing of dangling bonds on single dimers.[16] Si(001):D TPD spectra are well fit (excluding the narrow region at low θ_D and high T_s noted above) using standard Polanyi-Wigner analyses yielding activation energies E_a and prefactors ν of 1.88 eV and 1×10^{13} s^{-1} for β_2 and 2.52 eV and 1×10^{15} s^{-1} for β_1.[14] With increasing Ge coverage, the low- and high-temperature features initially broaden and shift to lower temperatures. Following Ref. 8, all Ge-adsorbed spectra were fit with four second-order peaks corresponding to

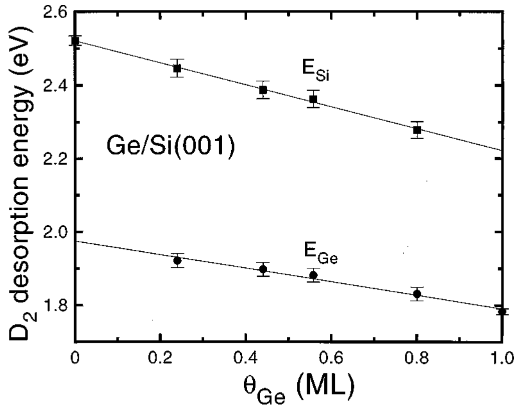

FIG. 2. Deuterium desorption activation energies E_{Si} and E_{Ge} from Si and Ge sites as a function of the Ge coverage θ_{Ge} on Ge-adsorbed Si(001) surfaces.

D_2 desorption from, beginning at the lowest temperature, Ge monodeuteride dimers (α), Si dideuteride atoms (β_2), mixed Si-Ge monodeuteride dimers (β_1'), and Si monodeuteride dimers (β_1).

Ge coverages were quantitatively determined by two separate techniques. The first was to use the integrated α, β_1, and β_1' monodeuteride TPD intensities following the procedure discussed in Ref. 8. The total intensity I_Σ under the three monohydride peaks is directly proportional to the substrate surface atom density N_s. Thus, setting $I_\Sigma = 1$ ML, θ_{Si} and θ_{Ge} are given by $(I_{\beta_1}+0.5I_{\beta_1'})$ and $(I_\alpha+0.5I_{\beta_1'})$, respectively. This results in $\theta_{Ge}=0.24$, 0.43, and 0.80 ML for the samples corresponding to Figs. 1(b)–1(d). We also employed AES, utilizing the escape depth and sensitivity factors given in Refs. 17 and 18, to obtain $\theta_{Ge}=0.25$, 0.42, and 0.80 ML. A similar good agreement was obtained for all samples, including the $Si_{1-x}Ge_x$ alloy layers, which were shown by high-resolution x-ray diffraction to be fully strained (thus, the sum of the monodeuteride TPD intensities remained proportional to N_s).

The temperatures of all four peaks in Ge-adsorbed Si(001) TPD spectra decreased with increasing θ_{Ge}, in agreement with previous qualitative observations for which absolute values of θ_{Ge} were unknown,[9] indicating that the deuterium desorption energy from Si (Ge) sites decreases (increases) with increasing Ge (Si) concentration. Since α, corresponding to D_2 desorption from Ge monodeuteride, has the lowest activation energy, the observed increase in the α peak temperature with decreasing θ_{Ge} must be due to the presence of Si strengthening the Ge-H bond while the decrease in the β_1 and β_2 peak temperatures indicates that Ge weakens the Si-H bonds.

TPD spectra from all Ge-adsorbed Si(001) samples were fit using the same frequency factors for β_1 ($\nu_{Si}=1\times10^{15}$ s^{-1}) and α ($\nu_{Ge}=5\times10^{14}$ s^{-1}) that we obtain for D_2 desorption from pure Si(001) and Ge(001), surfaces, respectively. The fits in all cases were at least as good as those in Figs. 1(b)–1(d). Figure 2 shows that the D_2 desorption energies for monodeuteride β_1 and α, E_{Si} and E_{Ge}, decrease linearly with increasing θ_{Ge}. From least-squares analyses, $E_{Si}=[E_{Si}(\mathrm{Si})-0.30\theta_{Ge}]$ eV and $E_{Ge}=[E_{Ge}(\mathrm{Ge})+0.17(1-\theta_{Ge})]$ eV, where $E_{Si}(\mathrm{Si})=2.52$ eV and $E_{Ge}(\mathrm{Ge})=1.80$ eV are the pure Si(001) and Ge(001) desorption energies.

A typical D_2 reference TPD spectrum from a clean Ge surface is reproduced in Fig. 3(a). It consists of a peak centered at 310 °C, due to desorption from the Ge monodeuteride α phase, with a shoulder at 260 °C arising from the presence of a small concentration of Ge dideuteride.[19] Figure 3(a) also contains TPD results from a partial-monolayer Si-adsorbed Ge(001) sample. The Si_2H_6 dosing, a 3-min expo-

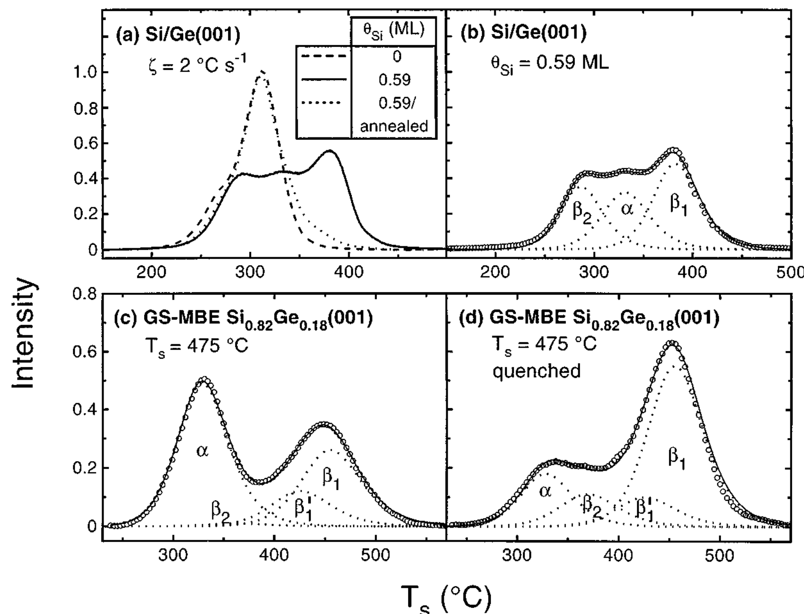

FIG. 3. (a) D_2 TPD spectra from Ge(001) and a Si-adsorbed Ge(001) surface with Si coverage $\theta_{Si}=0.59$ ML. The adsorbed-layer sample was prepared by Si_2H_6 dosing with $J_{Si_2H_6}=2.2\times10^{16}$ cm^{-2} s^{-1} for 3 min at 250 °C. A spectrum obtained from the $\theta_{Si}=0.59$ ML sample after *in situ* annealing at 600 °C for 30 s is also shown. (b) Fitted $\theta_{Si}=0.59$ ML D_2 TPD spectrum from (a). (c) D_2 TPD spectrum from a GS-MBE $Si_{0.82}Ge_{0.18}$(001) layer grown at $T_s=475$ °C. (d) As in (c) except that the film was immediately quenched to <200 °C in <20 s following growth.

sure to a flux of 2.2×10^{16} cm^{-2} s^{-1}, was carried out at 250 °C, after which the sample was immediately quenched to <200 °C in <20 s in order to minimize Si/Ge(001) surface site exchange. The TPD spectrum consists of three peaks. Consistent with the Ge-adsorbed Si(001) results above and previous GS-MBE $Si_{1-x}Ge_x$ TPD spectra,[8] we assign the high-temperature peak near 380 °C primarily to D_2 desorption from Si monodeuteride with a small contribution from mixed Si-Ge dimers, the middle peak at 330 °C to Ge monodeuteride, and the low-temperature peak at 290 °C to a mixture of Si and Ge dideuteride. If we assume that the high-temperature peak is entirely due to Si dimers, we obtain a Si coverage of 0.59 ML, in reasonable agreement with AES results yielding 0.55 ML. The fitted spectrum exhibits excellent agreement with the experimental data as shown in Fig. 3(b).

Comparing the Fig. 3(b) TPD results from Si-adsorbed Ge(001) ($\theta_{Ge}=0.41$ ML) with those in Fig. 1(c) for Ge-adsorbed Si(001) at approximately the same average surface composition, $\theta_{Ge}=0.43$ ML, shows a large shift in the position of the Si monodeuteride and dideuteride peaks. We focus on monodeuteride desorption since it is rate limiting during the low-temperature surface-reaction-controlled gas-source growth of $Si_{1-x}Ge_x$. The peak temperature $T_{\beta 1}$, which is $\simeq$470 °C for the Ge-adsorbed Si(001) sample [compared to 515 °C from clean Si(001)] decreases to 380 °C for Si-adsorbed Ge(001). This large decrease in $T_{\beta 1}$ cannot be explained by deuterium diffusing from Si sites to Ge and then desorbing from there since both samples have essentially the same Ge coverage. In fact, the present results imply that $T_{\beta 1}$, and hence the D-Si binding energy, is, in addition to being sensitive to the average surface layer composition (see Fig. 1), also a function of the second-layer composition.

Similarly, although the effect is smaller, the α peak position increases from 310 °C for clean Ge(001) [Fig. 3(a)] to 330 °C for Si-adsorbed Ge(001) [Fig. 3(b)] to 340 °C for Ge-adsorbed Si(001) [Fig. 1(c)], both of the latter samples with $\theta_{Ge}\simeq0.43$ ML. Thus, the D-Ge binding energy is also a function of both surface and second-layer composition.

A conceivable alternative explanation for the large shift in $T_{\beta 1}$ between Figs. 1(c) and 3(b) is continuous Ge enrichment at the surface of the Si-adsorbed Ge(001) sample due to segregation *during* the TPD measurement itself. This seems rather unlikely, however, since we have previously shown that significant Ge segregation requires temperatures well above 400 °C,[8] which is higher than the measured $T_{\beta 1}$ value for Si-adsorbed Ge(001). Moreover, all of the Si dangling-bond sites are filled with D, which we have shown strongly reduces the segregation enthalpy.[8] In addition, if Ge segregation during the measurement were the dominant channel leading to the observed decrease in $T_{\beta 1}$, we would expect a dramatic increase in peak asymmetry toward higher temperatures, but this is not observed. Thus, we conclude that the primary reason for the β_1 temperature shift between the samples in Figs. 1(c) and 3(b) is the difference in the composition of the second layer leading to long-range interactions.

The effects of Ge segregation can, however, be observed following high-temperature postdeposition annealing. Figure 3(a) shows TPD results obtained after *in situ* UHV annealing, for 30 s at 600 °C, the as-deposited ($\theta_{Si}=0.59$ ML) and quenched Si-adsorbed Ge(001) sample and resaturating the surface with deuterium. The spectrum is nearly identical to that obtained from the clean Ge surface with the exception of a small tail, due to some residual Si monohydride, toward higher temperatures. Continued annealing for another minute removes the tail completely and yields the original spectrum. Thus, the anneals result in essentially complete site exchange between adsorbed Si and second-layer Ge atoms.

Figure 3(c) is a D_2 TPD spectrum from a 200-nm-thick as-deposited fully strained $Si_{0.82}Ge_{0.18}$ film grown at $T_s=475$ °C (deposition rate$=0.2$ ML s^{-1}) and held at this temperature for $\simeq$30 s after the gases were valved off before being slowly cooled to room temperature. The thermal hold ensures that deposition which takes place while residual precursor gas is being purged from the chamber occurs at the desired growth temperature. This was tested by repeating the experiment using the same growth procedure but with the layer held at T_s for 5 min after valving off the gases. The TPD results are identical. Both sets of spectra are well fit, as in the Ge-adsorbed Si(001) case, using four peaks: α Ge monohydride, β_2 Si dihydride, β_1' mixed Si-Ge dimer monohydride, and β_1 Si monohydride. The peak temperatures are $T_\alpha=330$ °C, $T_{\beta 2}=365$ °C, $T_{\beta 1'}=430$ °C, and $T_{\beta 1}=455$ °C. Based upon the integrated monohydride peak intensities, $\theta_{Ge}=0.62$ ML. This is in excellent agreement with the steady-state value of 0.63 calculated based upon the Ge segregation enthalpy corresponding to $x=0.18$ and $T_s=475$ °C (steady-state H coverage $\theta_H=0.43$ ML).[8]

A TPD spectrum obtained from a $Si_{0.82}Ge_{0.18}$ film that was grown under conditions identical to sample 3(c), but thermally quenched ($T_s<200$ °C in <15 s) immediately upon valving off the source gases is shown in Fig. 3(d). In this case, the Ge surface coverage was only $\simeq$0.3 ML since the upper layer was formed from residual source gas chemisorbed during the quench and Ge-Si site exchange was strongly inhibited at the reduced temperatures. However, even though θ_{Ge} is lower by a factor of two, Fig. 3(d) shows that $T_{\beta 1}$ is $\simeq$455 °C, nearly equal to the value obtained from sample 3(c) with $\theta_{Ge}=0.62$ ML. This is yet another manifestation of the effect of second-layer composition on H desorption kinetics. That is, for sample 3(c), the second-layer composition is expected to be less than that of the bulk, $x=0.18$, due to strong surface segregation while for the quenched sample, the second-layer composition is closer to $x=0.6$. Thus, the large increase in second-layer Ge concentration between samples 3(d) and 3(c) compensates for the decrease in Ge surface coverage. The net result is an approximately constant value of $T_{\beta 1}$.

As a final example of the dependence of H desorption energy on underlayer composition, compare the TPD spectrum from a Ge-adsorbed Si(001) sample with $\theta_{Ge}=0.24$ ML shown in Fig. 1(b) to that of the quenched alloy in Fig. 3(d). Both have essentially the same Ge coverage. $T_{\beta 1}$ for sample 1(b) (490 °C) is higher, however, since the second-layer Ge concentration is much less than that of sample 3(d) ($T_{\beta 1}=455$ °C).

An additional set of D_2 TPD experiments was carried out on Ge-adsorbed Si(001) and $Si_{1-x}Ge_x(001)$ surfaces with low D coverages.[20] The resulting spectra, shown in Fig. 4(a), exhibit only β_1, with no associated α peaks, and the β_1 features occur at the same positions as those obtained follow-

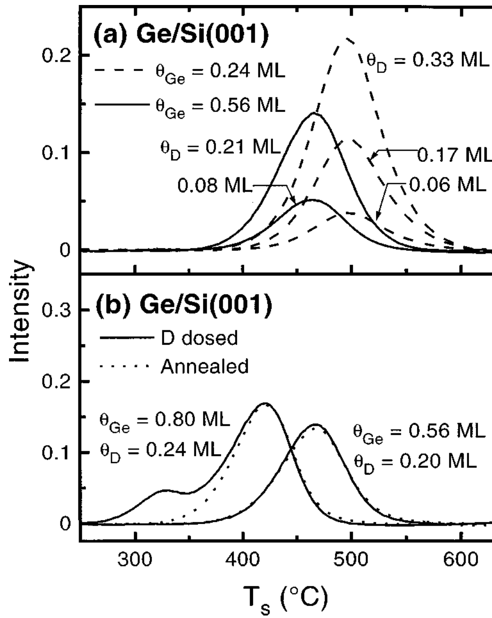

FIG. 4. D_2 TPD spectra from Ge-adsorbed Si(001) surfaces dosed with deuterium to yield (a) $\theta_{Ge}=0.24$ ML with $\theta_D=0.06$, 0.17, and 0.33 ML and $\theta_{Ge}=0.56$ ML with $\theta_D=0.08$ and 0.21 ML (b) D_2 TPD spectra from Ge-adsorbed Si(001) surfaces dosed with deuterium to yield $\theta_{Ge}=0.56$ ML with $\theta_D=0.20$ ML and $\theta_{Ge}=0.80$ ML with $\theta_D=0.24$ ML. The dotted lines are the corresponding spectra after *in situ* annealing at 380 °C ($\theta_{Ge}=0.56$ ML) and 330 °C ($\theta_{Ge}=0.80$ ML) for 30 s.

ing D saturation. Since the monodeuteride binding energy is higher on Si (2.52 eV) than on Ge (1.80 eV) sites and D is highly mobile at both the D dosing (200 °C) and initial ramping temperatures with a diffusion energy[21–23] lower than either desorption energy, deuterium will migrate preferentially to available Si sites. This, in turn, results in preferential desorption from Si sites as observed.

Figure 4(b) shows TPD spectra from Ge-adsorbed Si(001) samples with $\theta_{Ge}=0.56$ and 0.80 ML which were dosed with deuterium under identical conditions to provide similar coverages θ_D of 0.20 and 0.24 ML, respectively. Consistent with the results in Fig. 4(a) and Ref. 20, the $\theta_{Ge}=0.56$ ML spectrum exhibits only a Si monodeuteride β_1 peak while the $\theta_{Ge}=0.80$ ML spectrum also contains a small low-temperature Ge monodeuteride α peak. The $\theta_{Ge}=0.56$ ML sample was annealed at 380 °C and the $\theta_{Ge}=0.80$ ML sample at 330 °C, both for 30 s. The samples were immediately quenched and reanalyzed by TPD. The results show that annealing led to a loss of the small α peak in the $\theta_{Ge}=0.80$ ML sample spectra but no significant change in either of the β_1 peaks. If the primary hydrogen desorption pathway from Si sites involves deuterium diffusion from Si to Ge followed by desorption from Ge sites as previously proposed,[10,11] then the Si monodeuteride peaks should decrease since the annealing temperature was above the Ge monohydride desorption temperature for these samples, 335 and 320 °C, respectively. However, the results are in agreement with the conclusions deduced from Fig. 4(a) in which the majority of the deuterium is trapped at the higher-binding-energy Si sites and desorbs from there.

The data in Figs. 4(a) and 4(b) illustrate another point. As in the case of deuterium-saturated Ge-adsorbed Si(001) surfaces, β_1 peak positions from samples with a constant low D coverage decrease in temperature with increasing θ_{Ge}. An analysis of these and similar spectra shows that $T_{\beta 1}$ decreases by approximately 1 °C per 0.01 ML of Ge.

IV. DISCUSSION

The above results provide insight into the primary reaction path leading to H desorption from $Si_{1-x}Ge_x(001)$ surfaces during hydride gas-source film growth in the low-temperature surface reaction-limited regime. Crystal growers have known for many years that $Si_{1-x}Ge_x$ deposition rates are higher than those for Si due to the higher steady-state dangling bond densities, and hence precursor reactive sticking rates, on $Si_{1-x}Ge_x$ caused by more rapid H desorption rates. Two primary pathways have been proposed for this. The first involves diffusion of H from Si (higher binding energy) to Ge (lower binding energy) sites followed by desorption from the Ge centers.[10,11] The other proposal is that the presence of Ge neighbors weakens the H-Si bond energy E_{Si}.[9] In the present research, we have demonstrated conclusively that the second case is correct. That is, for Ge-adsorbed Si(001), E_{Si} decreases linearly with increasing θ_{Ge} following the relationship $E_{Si}=(2.52-0.30\theta_{Ge})$ eV. Similarly, E_{Ge} varies as $(1.80+0.17[1-\theta_{Ge}])$ eV. This results from electronic interactions that reflect the effect of Ge (Si) alloying on the Si (Ge) band structure[24] and, hence, on local bond energies. We have also shown that, as would be expected from these arguments, E_{Si} is dependent not only upon the composition of lateral in-plane neighbors, but upon the average composition of second-layer neighbors as well. We find that the D-Si binding energy is more sensitive to the presence of Ge than the D-Ge energy is to Si. This is consistent with the electronic structure of strained $Si_{1-x}Ge_x$ in which the rate of change in the Si Δ conduction-band minimum with increasing x is larger than that of Ge with increasing $(1-x)$.[24]

We now return to the issue of the nature of the H desorption site leading to the rate limiting step controlling film growth. Normal $Si_{1-x}Ge_x$ film growth temperatures, 400–600 °C, are well above H desorption temperatures T_α. Moreover, the D_2 TPD results for undersaturated $Si_{1-x}Ge_x$ surfaces in Fig. 4 show that D is preferentially trapped at, and is desorbed from, Si sites during thermal ramping. Thus, the rate-limiting step for low-temperature $Si_{1-x}Ge_x$ growth from hydrides is H desorption from Si, rather than Ge, sites as had been previously proposed.

Finally, we note that our E_{Si} and E_{Ge} values as a function of θ_{Ge} for Ge-adsorbed Si(001) are in very good agreement with our previous $E_{Si}(\theta_{Ge})$ and $E_{Ge}(\theta_{Ge})$ measurements from GS-MBE $Si_{1-x}Ge_x$ layers grown from Si_2H_6/Ge_2H_6 mixtures.[8] In the latter case, the θ_{Ge} values included the very strong effect of Ge surface segregation. Since we have shown in the present work that E_{Si} and E_{Ge} are also sensitive to the underlayer composition, this suggests that the average concentration of the second layer in growing $Si_{1-x}Ge_x$ films is very Si rich. There is some evidence for such an effect, a Ge-enriched overlayer on a Ge-deficient second layer, in solid-source MBE $Si_{1-x}Ge_x(001)$ films examined by angular-resolved photoemission.[25] Moreover, it was actually predicted earlier based upon combined surface energy and

elastic strain considerations.[26,27] The Ge surface energy is approximately 0.07 eV/atom less than that of Si while its covalent radius is 4% larger.

V. CONCLUSIONS

The rate-limiting step for the gas-source hydride growth of $Si_{1-x}Ge_x(001)$ in the low-temperature surface-reaction-limited regime is hydrogen desorption from Si monohydride species. We have used D_2 TPD measurements on Ge-adsorbed-Si(001), Si-adsorbed Ge(001), and $Si_{1-x}Ge_x(001)$ to show that this occurs directly from Si sites rather than through the previously postulated two-step process of diffusion to lower-binding energy Ge surface sites and desorption from there. However, the H monohydride binding energy E_{Si} at Si sites decreases rapidly with increasing Ge concentration in both the growing overlayer *and* the underlayer (i.e., with the average overall concentration of Ge near neighbors). Similarly, the H monohydride binding energy E_{Ge} at Ge sites increases with the average overall concentration of Si near neighbors. For adsorbed Ge layers on Si(001), we find that $E_{Si}=(2.52-0.30\theta_{Ge})$ eV while $E_{Ge}=(1.80+0.17[1-\theta_{Ge}])$ eV.

These results imply that the activation energy for surface-reaction-controlled $Si_{1-x}Ge_x$ growth should be equal to $E_{Si}(\theta_{Ge})$ where θ_{Ge} is the steady-state Ge surface coverage including segregation and we assume that the second-layer is Ge deficient and nearly pure Si. Incorporating these results in a model describing $Si_{1-x}Ge_x$ growth rate kinetics as a function of x and T_s provides very good agreement with experimental data.[28]

ACKNOWLEDGMENTS

The authors gratefully acknowledge the financial support of the Office of Naval Research through Contract No. NOOO14-96-1-0280 administered by Dr. Larry Cooper and the Semiconductor Research Corporation.

[1] Q. Lu, M. R. Sardela, Jr., T. R. Bramblett, and J. E. Greene, J. Appl. Phys. **80**, 4458 (1996).

[2] G. Abstreiter, H. Brugger, T. Wolf, H. Jorke, H. J. Herzog, Phys. Rev. Lett. **54**, 2441 (1983).

[3] E. Kasper, J. Cryst. Growth **150**, 921 (1995).

[4] T. P. Pearsall, J. C. Bean, R. People, and A. T. Fiory, *Proceedings of the 1st International Symposium on Si MBE* (ECS, Penington, NJ, 1983), p. 366.

[5] K. Ismail, S. Richton, and J. O. Cho, IEEE Electron Device Lett. **14**, 348 (1993); S. J. Koester, K. Ismail, and J. O. Cho, Appl. Phys. Lett. **70**, 2422 (1997).

[6] R. People, IEEE J. Quantum Electron. **22**, 1696 (1986).

[7] H. Hirayama, T. Tatsumi, and N. Aizaki, J. Cryst. Growth **95**, 476 (1989).

[8] H. Kim, N. Taylor, J. R. Abelson, and J. E. Greene, J. Appl. Phys. **82**, 6062 (1997).

[9] B. M. H. Ning and J. E. Crowell, Surf. Sci. **295**, 79 (1993).

[10] Y. M. Wu, J. Baker, P. Hamilton, and R. M. Nix, Surf. Sci. **295**, 133 (1993).

[11] B. S. Meyerson, K. J. Uram, F. K. LeGoues, Appl. Phys. Lett. **53**, 2555 (1988).

[12] Q. Lu, T. R. Bramblett, N.-E. Lee, M.-A. Hasan, T. Karasawa, and J. E. Geene, J. Appl. Phys. **77**, 3067 (1995).

[13] X.-J. Zhang, G. Xue, A. Agarwal, R. Tsu, M.-A. Hasan, J. E. Greene, and A. Rockett, J. Vac. Sci. Technol. A **11**, 2553 (1993).

[14] H. Kim, G. Glass, S. Y. Park, T. Spila, N. Taylor, J. R. Abelson, and J. E. Greene, Appl. Phys. Lett. **69**, 3869 (1996).

[15] U. Höfer, L. Li, and T. F. Heinz, Phys. Rev. B **45**, 9485 (1992).

[16] J. J. Boland, J. Vac. Sci. Technol. A **10**, 2458 (1992).

[17] C. C. Chang, Surf. Sci. **48**, 9 (1975).

[18] L. E. Davis, N. C. McDonald, P. W. Palmberg, G. E. Riach, and R. E. Weber, *Handbook of Auger Electron Spectroscopy*, 2nd ed. (Physical Electronics Industries, Flying Cloud, MN, 1976).

[19] H. Kim and J. E. Greene (unpublished).

[20] ''Low'' deuterium coverage as used in this context depends upon the Ge coverage and varies from, for example, <0.20 ML with $\theta_{Ge}=0.56$ ML to <0.33 ML with $\theta_{Ge}=0.24$ ML.

[21] A. Vittadini, A. Selloni, and M. Casarin, Surf. Sci. **289**, L625 (1993).

[22] C. J. Wu, I. V. Ionova, and E. Carter, Phys. Rev. B **49**, 13 488 (1994).

[23] J. H. G. Owen, D. R. Bowler, C. M. Goringe, K. Miki, and G. A. D. Briggs, Phys. Rev. B **54**, 14 153 (1996).

[24] C. G. Van de Walle and R. M. Martin, Phys. Rev. B **34**, 5621 (1986).

[25] J. E. Rowe, D. M. Riffe, G. K. Wertheim, and J. C. Bean, Appl. Phys. Lett. **76**, 4915 (1995).

[26] P. C. Kelires and J. Tersoff, Phys. Rev. Lett. **63**, 1164 (1990).

[27] P. C. Weakliem and E. Carter, Phys. Rev. B **45**, 13 458 (1992).

[28] H. Kim, N. Taylor, T. Bramblett, and J. E. Greene (unpublished).